

Theoretical Gas Flow through Gaps in Screw-type Machines

Prof. Dr.-Ing. K. Kauder, Dipl.-Ing. D. Stratmann

University of Dortmund, Fachgebiet Fluidenergiemaschinen

(The experimental part of these studies was promoted by the German Research Foundation DFG)

Abstract

The entire energy conversion as well as the operating reliability of positive displacement rotary machines is highly affected by leakage mass flows. Both computational fluid dynamics (CFD) and experimental flow visualisation plus velocity measurements with Layer-Two-Forwarding method are applied to investigate the gas flow in screw-type machines. The CFD-analysis of the gas flow in a male rotor-housing gap of a screw-type machine provides a first insight into flow physics shown in the experiment. Turbulence models of the CFD-software Fluent[®] are examined with a view to discovering how accurately it can simulate the gap flow.

1 Introduction

The global scientific intention to develop a realistic modelling of the process flow in dry-running screw-type machines is the reference framework for this paper. Characterising the gas flow in screw-type machines is the first step towards this longer term aim. The leakage mass flow and the impermeability of gaps respectively acquire greater significance also because of higher leakage mass flows in dry-running machines in comparison to wet-running screw-type machines. The clearances between the three main components of a screw-type machine – male rotor, female rotor and casing – should be minimised to achieve efficient energy conversion, otherwise the minimum operating clearance is determined by the deformation of the machine components, and thus the operating reliability, as the rotors must not make contact.

As a result of the direct relationship between the gas flow in screw-type machines and the operating behaviour flow, conditions of the machine type are investigated.

In addition to experimental flow research and analytical flow mechanics, computational fluid dynamics (CFD) has become more important in the last few years, closely linked to higher processor speeds, **fig. 1**. CFD is the science of determining a numerical solution to the governing equations of fluid flow (the set of *Navier-Stokes equations*, continuity and any additional conservation equations, for example energy or species concentrations), whilst advancing the solution through space or time to obtain a numerical description of the complete flow field of interest.

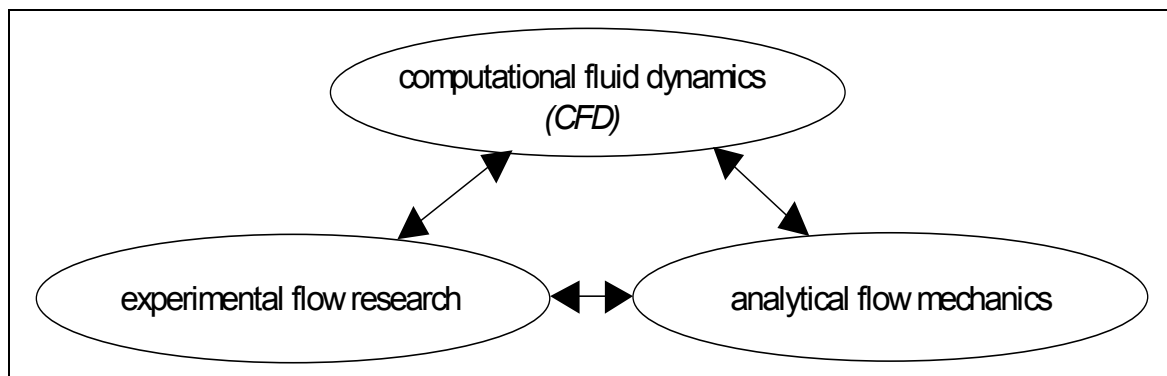


Fig. 1: Relation between the different fluid dynamic fields /1/

As the general scientific issue appears quite complex and extensive, an approach in stages using experiment and simulation in close interaction is chosen. This paper addresses the subordinate target of experimental and theoretical research into clearance flow in the rotor-to-housing gap in dry-running screw-type machines. In addition to the experimental investigation on a plane 1:1 screw-type machine model, the CFD-analysis of the clearance flow is presented. Simulation results are validated using

experimental flow visualisation via the Schlieren technique and velocity measurements by means of the Layer-Two-Forwarding method.

2 Experimental investigation of the clearance flow

As direct flow measurement in the gaps of real screw-type machines appears difficult to access and the working chamber flow can only be selectively measured with a laser anemometer, Kauder and Sachs have examined clearance flow using a plane 1:1 screw-type machine model with full-scale clearances and fixed or movable contours /2, 3, 4, 5, 6, 7/.

The plane contour sheets of the rotor contour of a 4+6 screw-type machine for visualisation of the gas flow in the male rotor housing gap with fixed contours as used in the experiment, are shown in **fig. 2**.

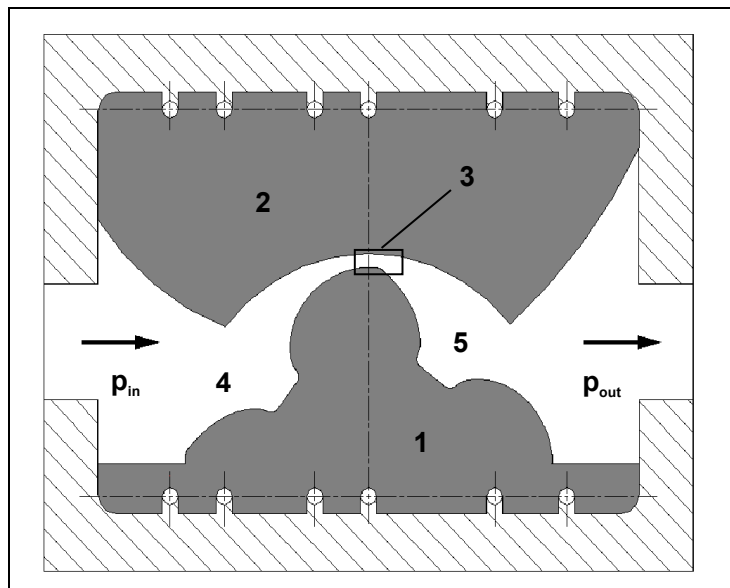


Fig. 2: Flow contours in the experiment /2/

- 1 male rotor
- 2 casing
- 3 male rotor-housing gap
- 4 leading working chamber
- 5 trailing working chamber

The flow situation represents an internal flow first with an increasing and then decreasing cross-section with fixed dimensions. The minimum clearances between rotor and casing are 0.1 to 0.4 mm. The clearance along the rotor-to-housing gap with one sealing strip is given in **fig. 3**. The male rotor has a sealing strip, which has a height of 0.1 mm.

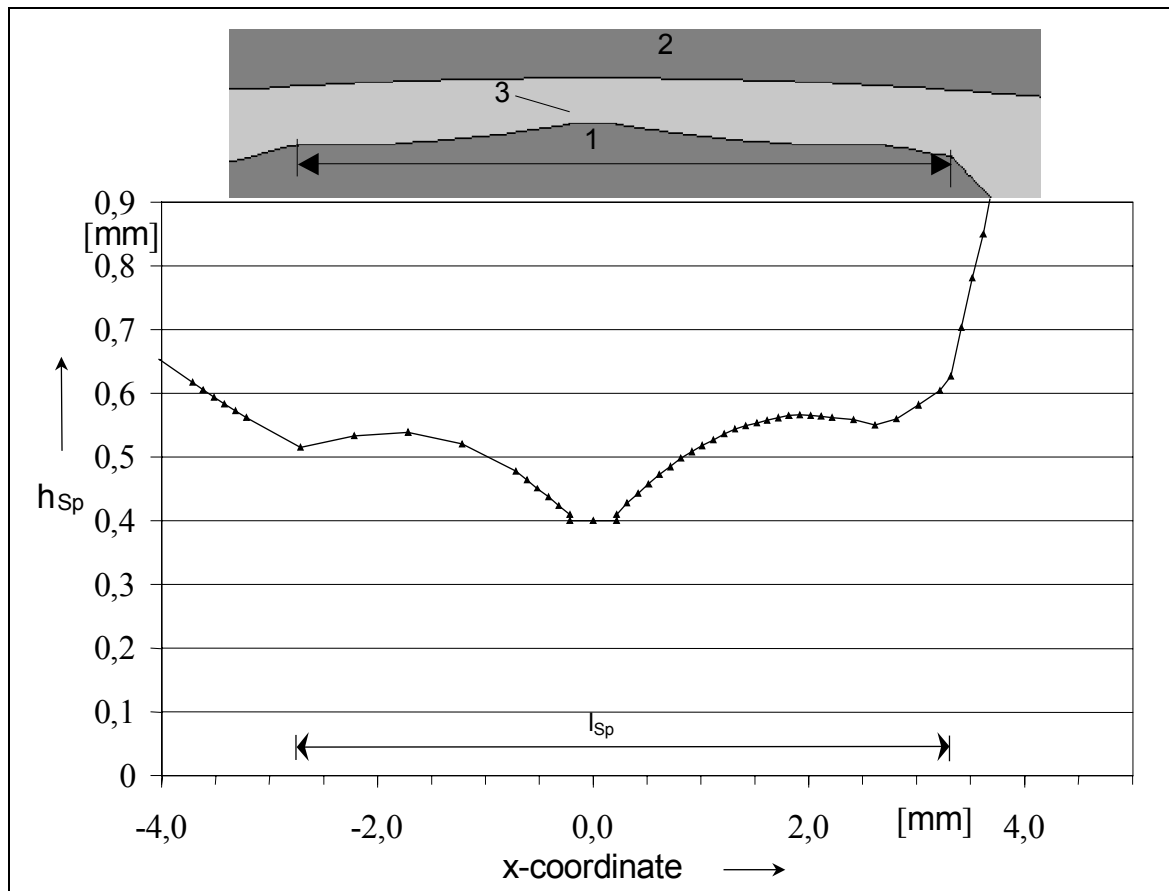


Fig. 3: Clearance h_{sp} along the male rotor-housing gap

- 1 male rotor
- 2 casing
- 3 sealing strip

The experimental flow visualisation reproduces density gradients using the Toepler Schlieren technique which does not affect the flow field. **Fig. 4** presents a Schlieren picture of the clearance flow in the screw-type machine model with total and enlarged views. Changes in tone correspond to density gradients in flow direction (from left to right), light areas representing density decrease (negative density gradient), dark areas representing density increase (positive density gradient). Due to the test arrangement, very strong negative density gradients are also represented by dark shades [8]. The experimental test results illustrate both the effect of pressure ratio in the wind tunnel (outlet to inlet pressure) and clearance on the flow conditions in the gap and, as predicted, on the trailing working chamber.

For a pressure ratio of $\Pi_W = \frac{p_{out}}{p_{in}} = 0.25$, a turbulent, partly unstable flow is shown in the gap. This has a significant influence on the flow conditions in the following working chamber downstream from the gap. Partly steady state shocks and shock structures are formed within the gap flow. As shown in fig. 4c a transonic shock is pro-

duced at the forward-facing step of the sealing strip, and indicates an extreme increase in flow velocity at the gap. The series of criss-cross shocks with separations also indicates a different heat transfer and flow rate, particularly in the gap.

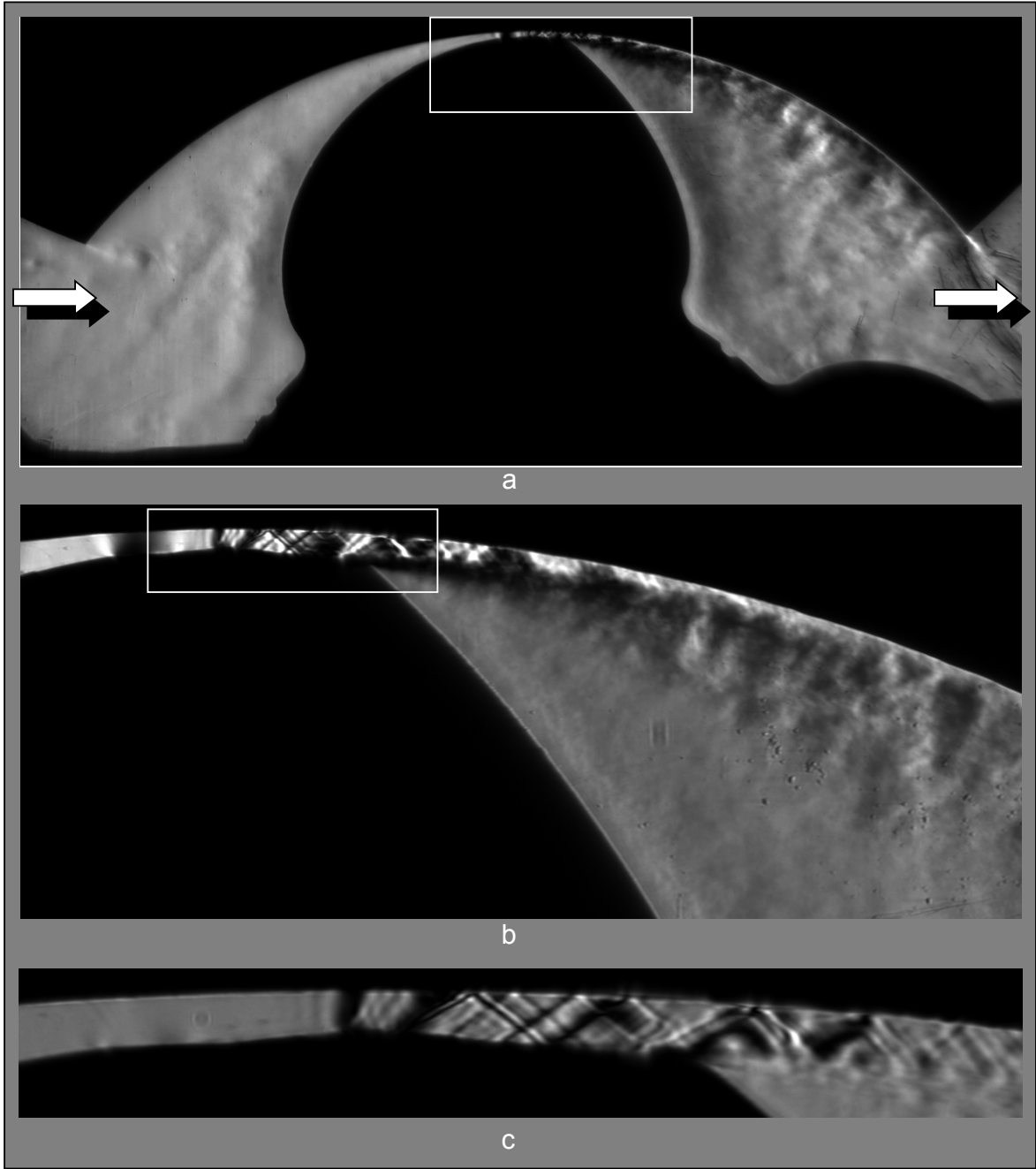


Fig. 4: Schlieren picture of the clearance flow at the single sealing strip; total view (a) and enlarged view (b and c); height of the gap $h_{Sp} = 0.4 \text{ mm}$; pressure ratio $II_W = 0.25$; exposure time $0.5 \mu\text{s}$ /7/

3 CFD analysing process

The fundamental principles of flow mechanics can be expressed in terms of mathematical equations, which in their most general form are usually partial differential equations (mass conservation, conservation of momentum and energy conservation). Computational Fluid Dynamics (CFD) is the science of determining a numerical solution to the governing equations of fluid flow whilst advancing the solution through space or time to obtain a numerical description of the complete flow field of interest. The governing equations for Newtonian fluid dynamics, the unsteady *Navier-Stokes equations*, have been known for over a century. However, the analytical investigation of reduced forms of these equations is still an active area of research as is the problem of turbulent closure for the Reynolds averaged form of the equations.

The simulation process can be divided into the following parts :

- **Preprocessing** : defining the computational domain; creation and design of the grid; setting of boundary conditions and physical properties; choice of turbulence model
- **Mainprocessing** : computational solution of the governing equation system
- **Postprocessing** : presentation and examination of simulation results
- **Validation** : critical review of simulation results, e.g. grid refinement to guarantee a grid independent solution; comparison with experimental data

The simulations are carried out using the CFD-code FLUENT[®]. The program offers several turbulence models for different application areas. Goals of this study are the examination of the abilities of different turbulence models of the CFD-software Fluent[®] to reproduce the gap flow close to reality.

4 Modeling the gap flow at the rotor-to-housing gap

4.1 Computational domain

The chosen computational domain, including the gap and the trailing working chamber corresponding to the experiment, is shown in **fig. 5**. A sufficient distance of the inlet to the gap guarantees minimum influence of inlet boundary conditions on the clearance flow and allows an analysis of the flow conditions at the forward gap. The outlet location was chosen downstream from the gap and the trailing working chamber to analyse the flow conditions there and to minimise back-flow influences on the computation.

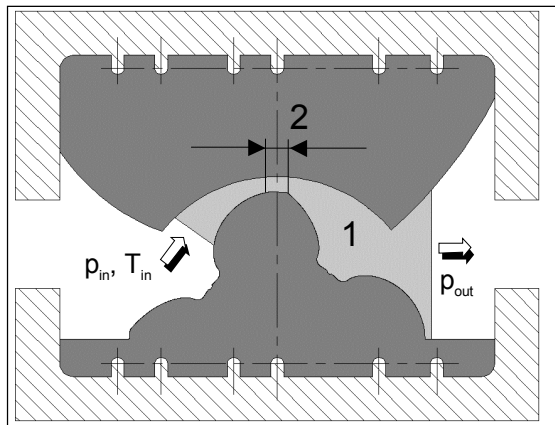


Fig. 5 : Flow contours and chosen computational domain

- 1 computational domain
- 2 gap length

The structured mesh consisting of 45.000 quadrilateral cells has an adequately higher density of nodes in the gap according for the purpose of investigating the clearance flow. To ensure a grid independent solution the simulations had also been performed with another mesh.

4.2 Boundary conditions and physical properties

To obtain a solution for the equation system, boundary conditions corresponding to the experiment are required.

Within the scope of this study a pressure ratio of $\Pi = 0.5$ with an inlet pressure of 2 bar and a minimum clearance of 0.4 mm is investigated. Two-dimensional steady-state calculations with fixed contours are presented. The streaming fluid is air and the flow is considered to be adiabatic. Further boundary conditions are shown in table 1.

medium	air
density	compressible
spec. thermal conductivity	$\mu = 1.82 \cdot 10^{-5} \text{ kg/ms}$
spec. thermal capacity	$c_p = 1006.43 \text{ J/kgK}$
roughness of walls	$k_s = 0$
movement of walls	$v = 0 \text{ m/s}$
heat transfer	adiabatic
minimum clearance	$h_{sp} = 0.4 \text{ mm}$
inlet	$p_{in} = 2 \text{ bar}$
	$T_{in} = 300 \text{ K}$
outlet	$p_{out} = 1 \text{ bar}$

Table 1: Summary of physical properties and boundary conditions

5 Simulation results

First numerical analyses of the clearance flow in the male rotor-to-housing gap of a screw-type machine were generated, using the CFD-code FLUENT[®], to compute the flow two-dimensionally and time independent with regard to compressibility.

5.1 Inviscid flow analyses

Inviscid flow analyses neglect the effect of viscosity on the flow resulting in a simplification of the calculations because viscous terms in the equation are ignored. Inviscid flow analyses are routinely used to provide a good initial solution for problems involving complicated flow physics and/or complicated flow geometry. For this the “initial solution” presents a extremal reflection of the flow situation ($Re \Rightarrow \infty$).

An overview of the investigated flow situation is given by the simulation result showing the whole computational domain. The distribution of flow velocity is made clear in **fig. 6**.

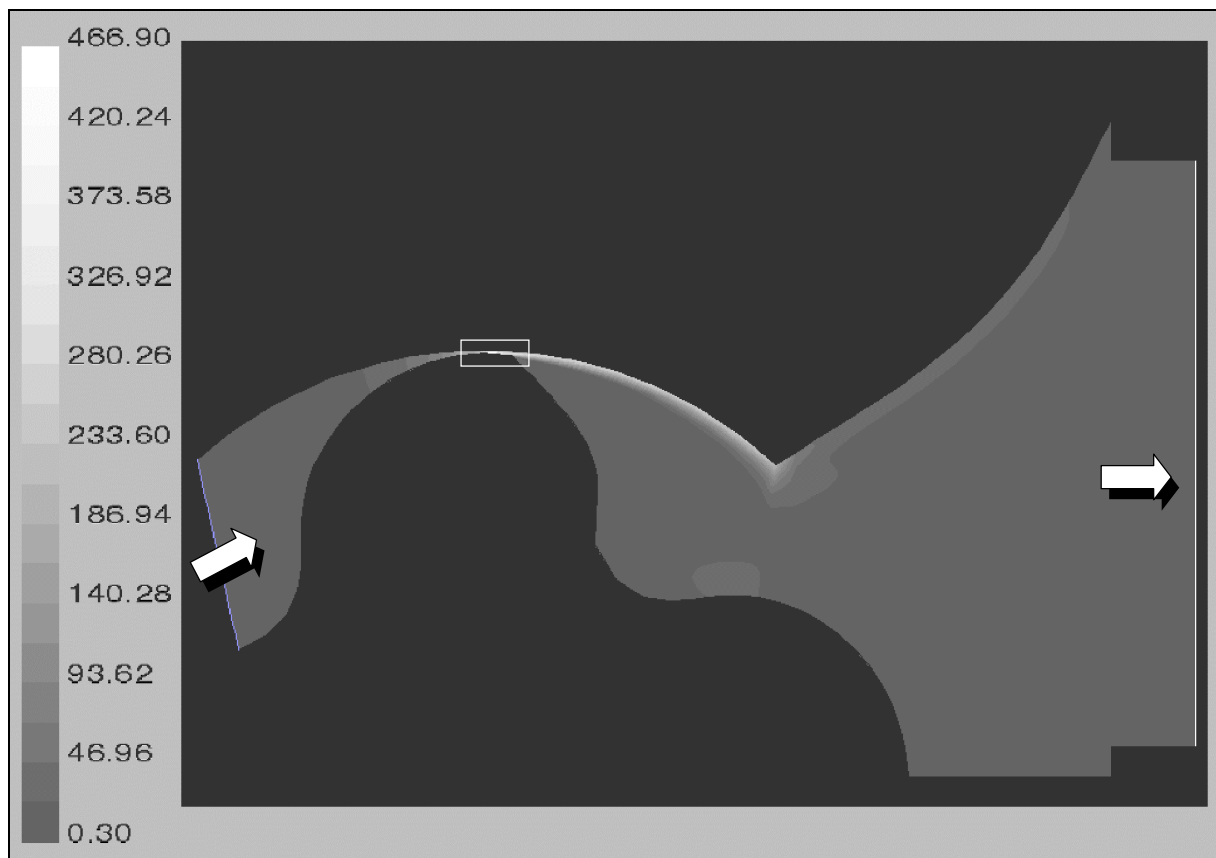


Fig. 6: *Flow velocity for the total zone, pressure ratio $\Pi_W = 0.5$; inlet pressure $p_{in} = 2$ bar; minimum clearance $h_{sp} = 0.4$ mm; inviscid model*

In the predominant area of the computational domain the flow velocity is calculated to be less than 30 m/s, while in the gap and in the trailing working chamber a significantly higher flow velocity is obtained. The flow is accelerated due to the converging

duct cross-section in the front gap and becomes supersonic in the gap downstream of the sealing strip. For the inviscid model the maximum flow velocity is 471 m/s and the maximum mach number 1.82. The transition point from subsonic to transonic flow is situated at the first forward-facing step of the sealing strip, **fig. 7**. The flow is deflected at the sealing strip, forming an expansion fan (Prandtl-Meyer expansion fan) and a separation bubble. At the centre of the sealing strip an oblique shock arises, starting the male rotor and reflected from the casing downstream. At the second, backward-facing step of the sealing strip, the supersonic flow separates from the rotor and is deflected, forming an expansion fan again while it is accelerated. The separated flow reattaches to the rotor and compression waves are formed that result in an oblique shock. Downstream this shock is also reflected from the casing wall.

The accelerated clearance flow does not follow the sharp-edged increasing cross-section at the ending of the gap because of its high energy level and separates from the rotor, forming a vortex in the trailing working chamber. The clearance flow continues streaming in the form of a jet adjacent to the casing wall.

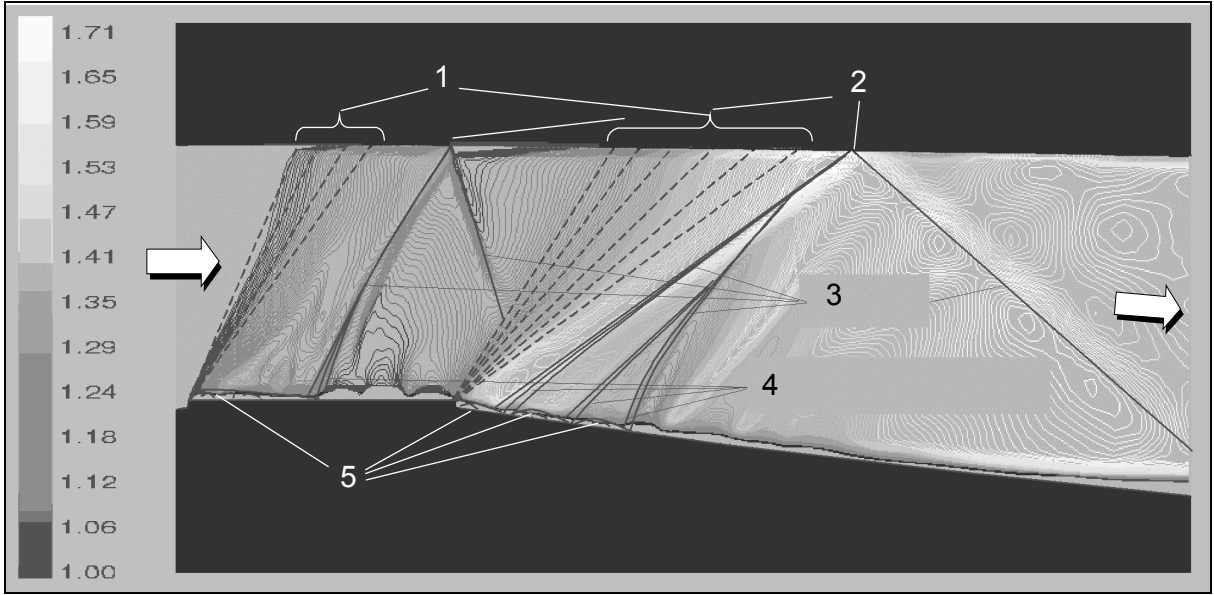


Fig. 7: *Flow situation at the sealing strip in the gap, showing the mach number distribution $Ma > 1$; pressure ratio $II_W = 0.5$, inlet pressure $p_{in} = 2$ bar; minimum clearance $h_{Sp} = 0.4$ mm; inviscid model*

- 1 expansion fan
- 2 shock reflection at the casing
- 3 shocks
- 4 compression waves
- 5 separation bubbles

5.2 Turbulence models

Turbulence models are termed according to the number of differential equations used to describe the flow, and are referred to as zero-, one- or two-equation models.

The CFD-Software FLUENT[®] provides one-equation model named the *Spalart-Allmaras model*. In its original form, the Spalart-Allmaras model is effectively a low-Reynolds-number model, requiring the viscous-affected region of the boundary layer to be properly resolved.

Differing simulation results are performed using the *Standard-k- ϵ turbulence model*. In this two-equation model the solution of two separate transport equations allows the turbulent velocity and length scales to be independently determined.

Showing the distribution of mach number contours for the local forming supersonic flow in the gap **fig. 8** presents simulation results for some computations using different turbulence models.

For the Spalart-Allmaras model the clearance flow becomes supersonic at the forward-facing step of the sealing strip of the male rotor (part a). Forming an expansion fan the supersonic flow is deflected at the backward-facing step of the sealing strip. As for the inviscid model there is an oblique shock starting from the rotor and reflected downstream by the casing wall. A maximum flow velocity of 467 m/s and a maximum mach number of 1.68 is assumed.

For the Standard-k- ϵ models using a “Two-Layer-Zonal” model that resolves the near wall region down to the wall including the viscous sublayer, the clearance flow is also accelerated from subsonic to supersonic speed at the forward-facing step of the sealing strip (part b). Differing from the described solution, the flow is decelerated to subsonic speed at the centre of the sealing strip. The flow is again accelerated to supersonic speed downstream and deflected at the backward-facing step of the sealing strip, forming an expansion fan and an oblique shock. The contours of the shock are not shown very sharply, in contrast to the Spalart-Allmaras model.

Part c presents the simulation result using the Standard-k- ϵ models and a wall function approach for the viscous sublayer, in which the viscous-affected region at the wall is not resolved, but bridged by semi-empirical formulas and functions. Differences to the above mentioned results are especially found at the forward-facing step of the sealing strip and in the gap downstream from the strip. The transonic point differs and jet-like structures are obtained for the end section of the gap, accelerating and decelerating the clearance flow. The mach number distribution along the gap for the different turbulence models is shown in **fig. 9**.

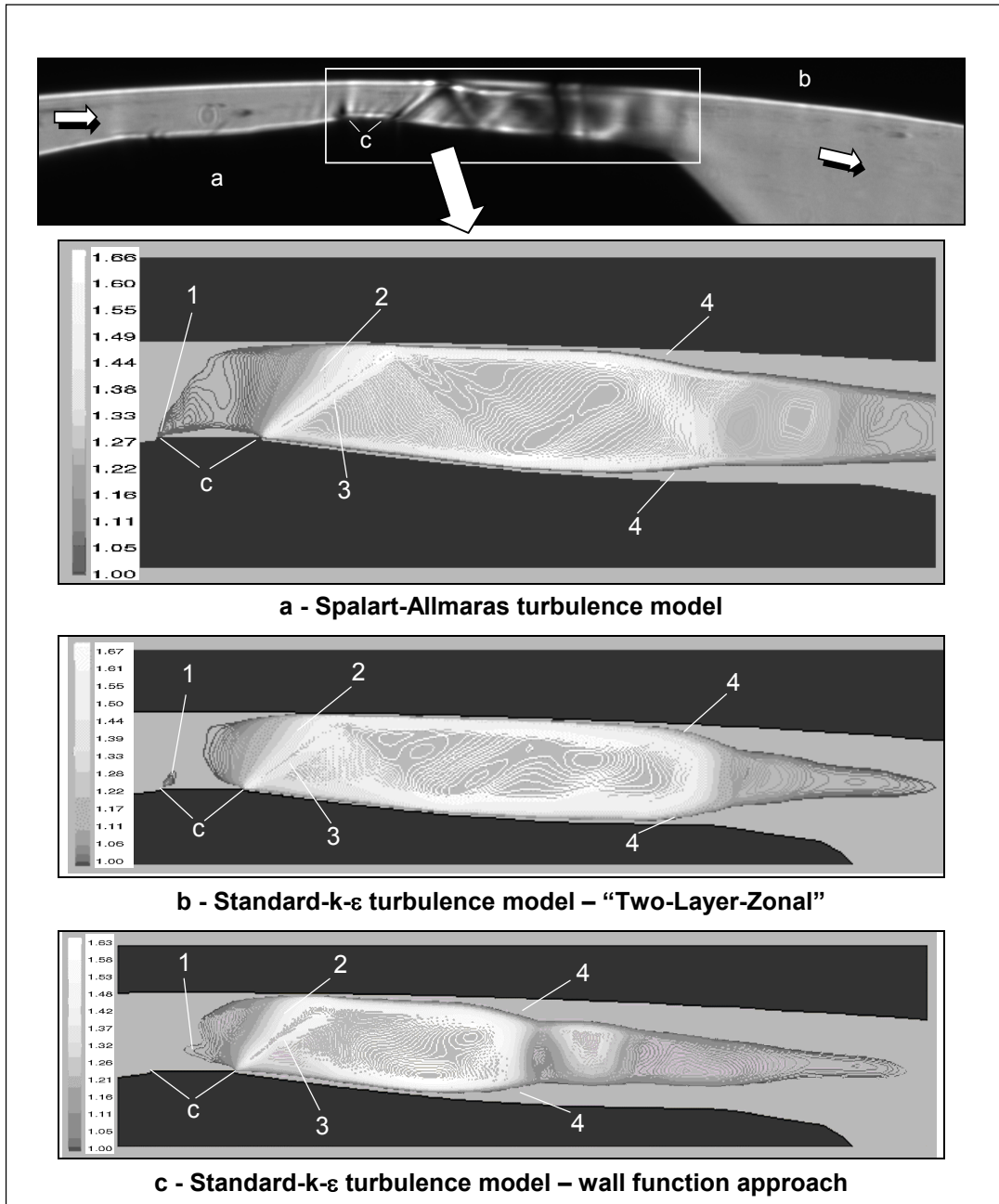


Fig. 8: Simulation results for different turbulence models; pressure ratio $\Pi_W = 0.5$, inlet pressure $p_{in} = 2$ bar; minimum clearance height $h_{Sp} = 0.4$ mm

- | | | | |
|---|------------------------------------|---|---------------|
| 1 | transition zone for transonic flow | a | male rotor |
| 2 | expansion fan | b | casing |
| 3 | oblique shock | c | sealing strip |
| 4 | separation and contraction | | |

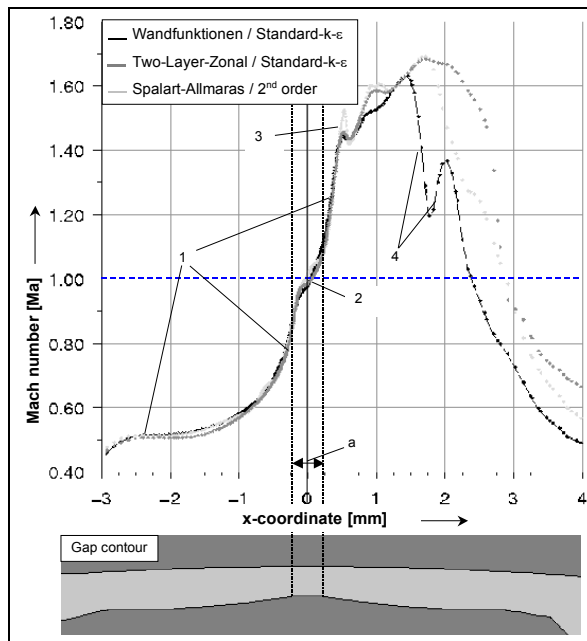


Fig. 9:

Mach number along the gap for different turbulence models; pressure ratio $\Pi_W = 0.5$; inlet pressure $p_{in} = 2$ bar; minimum clearance $h_{sp} = 0.4$ mm

- 1 nearly identical mach number curves in the gap upstream of the sealing strip
- 2 sonic flow at the throat of the gap
- 3 oblique shock downstream of the sealing strip
- 4 decelerated and accelerated flow in a complex pattern similar to jet streams downstream of the gap
- a sealing strip

6 Experiment and simulation by comparison

The characteristics of different turbulence models to reproduce the gap flow close to reality have to be checked, comparing them with experimental data as every turbulence model has strengths and weaknesses.

To make a comparison the computed supersonic flow field in the gap is compared in the form of mach number contours with Schlieren pictures, providing a qualitative insight into the flow conditions showing supersonic shocks or separations, **fig. 10**.

For the inviscid model the flow is blocked at the forward-facing step of the sealing strip. The transition point from subsonic to supersonic flow is also predicted to be located at the forward-facing step of the sealing strip. At the rear-facing step of the strip both computation and experiment indicate a deflected flow leading to an expansion fan, which results in an oblique reattachment shock starting from the rotor and reflected by the casing wall. Mach number contours and the oblique angle of the shock match each other in experiment and simulation. In contrast to the experiment, the shock induced separation from the casing wall downstream of the sealing strip shown in the Schlieren picture is not obtained by the calculation.

For the Spalart-Allmaras model the transition point is also predicted to be at the first step of the strip. An expansion fan does not form there similar to flow conditions shown by the Schlieren picture. The expansion fan forming at the backward-facing step of the strip and the oblique shock are indicated, as shown in the experiment. The shock contours are shown as sharply as on the flow picture. There are slight traces of a reflection of the shock from the casing in the mach number contours, but this is not as marked as in the results for the experiment. For the shock structure

downstream of the gap, the steady-state computation seems not be able to present the unstable flow conditions.

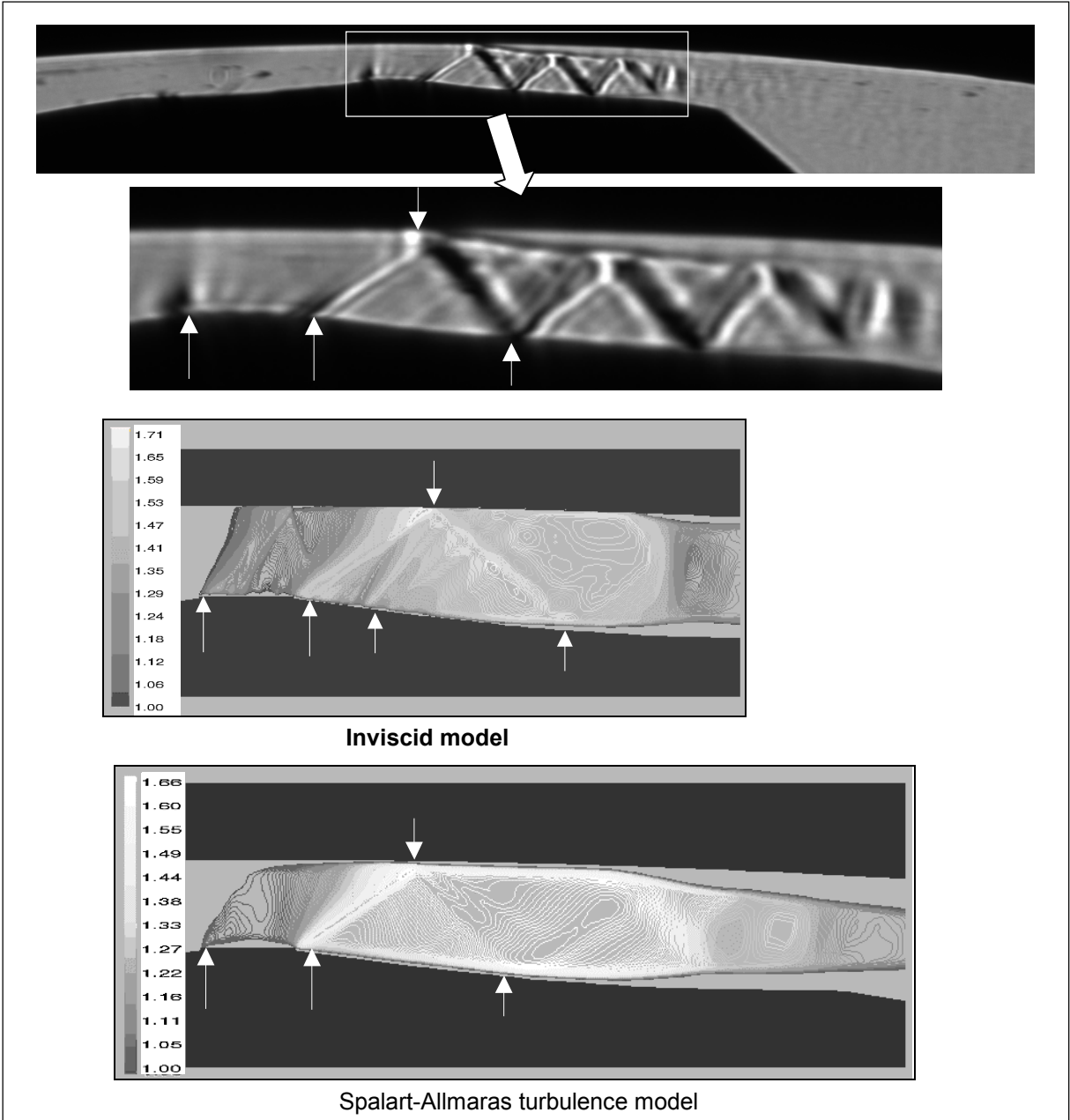


Fig. 10: Comparison between experimental Schlieren picture and simulation; pressure ratio $\Pi_w = 0.5$; inlet pressure $p_{in} = 2 \text{ bar}$; minimum clearance $h_{sp} = 0.4 \text{ mm}$

For a pressure ration of $\Pi_w = 0.33$ a comparison of the measured and calculated clearance flow velocity is given by **fig. 11**. The velocity gauged with Layer-Two-Forwarding method is lower than in the computation, specially asserted for supersonic flow downstream of the sealing strip. Sachs /8/ supposes that the particles drawn into the flow are not able to follow the strong local accelerations because of inertia.

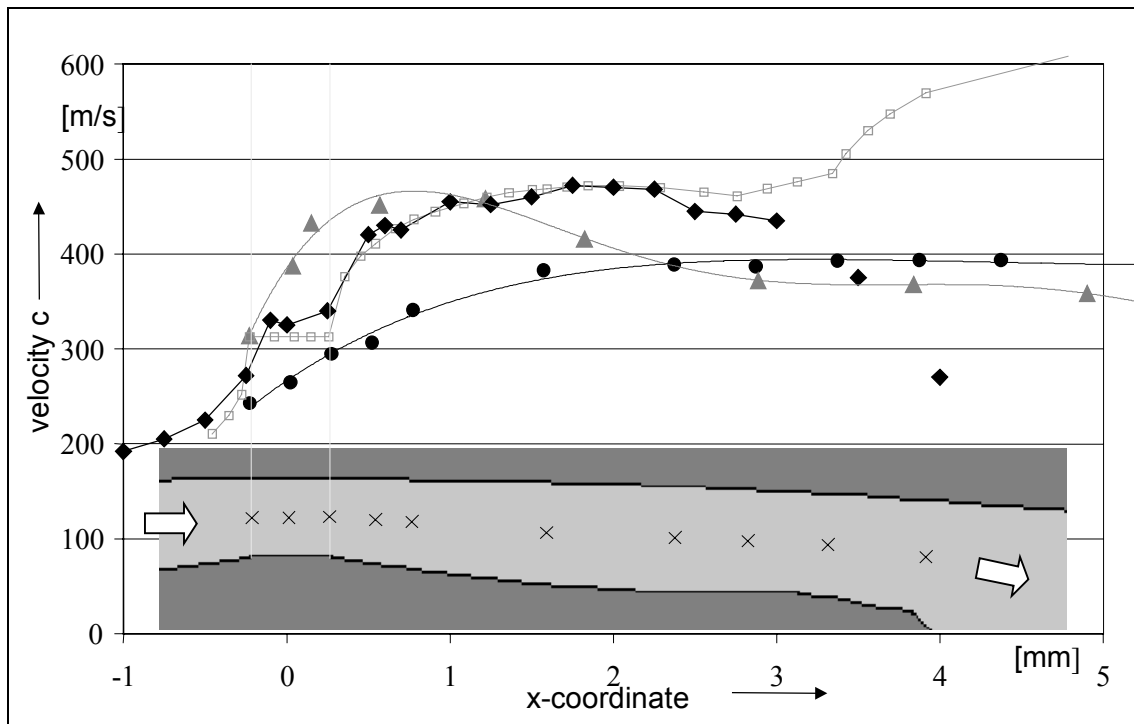


Fig. 11: Comparison of the flow velocity c in the experiment and the simulation; pressure ratio $\Pi_{W} = 0.33$; inlet pressure $p_{in} = 3 \text{ bar}$; minimum clearance $h_{sp} = 0.4 \text{ mm}$

- point: c by L2F-measurement
- triangle: c by mach number
- rhombus: c by CFD-calculation
- square: c for isentropic case

7 Outlook

An exact description of flow physics in screw-type machines is an extensive issue due to the complex flow conditions that promise to provide material for a long term research project. The presented studies offer a first step in computational fluid dynamics by analysing the clearance flow in the male rotor-to-housing gap. With regard to an improved and more realistic reproduction of the flow conditions shown in the experiment, an expansion to instationary computation is likely to be successful. Different operating conditions (variation in pressure ratio, clearance, sealing strip) need to be analysed with fixed and moving flow contours. Experimental data for validation do already exist in the form of the Schlieren picture.

For sufficient accuracy the computations should be used to analyse both the impermeability of gaps and the heat transfer between fluid and rotor as well as fluid and casing. In particular, the experimental investigation foreshadows different heat transfer characteristics from those assumed so far. The results obtained could be used for an extension of the program system simulating the operating behaviour of screw-type machines developed at the FG Fluidenergiemaschinen.

8 References

- /1/ **Wendt, J. E.** Computational Fluid Dynamics – An Introduction. Springer-Verlag, Berlin/Heidelberg, 1996
- /2/ **Kauder, K., Sachs, R., Araujo, L.** Experimental and numerical investigation of the gas flow using plane model of male rotor-housing gap in a screw-type machine. In: Schraubenmaschinen, Forschungsberichte des Fachgebietes Fluidenergiemaschinen Nr. 8, ISSN 0945-1870, pp 5-16, University of Dortmund, 2000
- /3/ **Kauder, K., Sachs, R.** Strömungen in arbeitsraumbegrenzenden Spalten von trockenlaufenden Schraubenmaschinen. In: VDI Berichte 1391, pp 107-130Düsseldorf: VDI-Verlag, 1998
- /4/ **Kauder, K., Sachs, R.** Gas Flow Research at a Plane Screw-Type Machine Model. Intern. Conference on Compressors and their Systems, pp 717-726, London: CITY University, IMechE Conference, Transactions, 1999
- /5/ **Kauder, K., Sachs, R.** Gas flow research at a plane screw-type machine model - Part 1. In: Schraubenmaschinen, Forschungsberichte des Fachgebietes Fluidenergiemaschinen Nr. 5, ISSN 0945-1870, pp 113-134, University of Dortmund, 1997
- /6/ **Kauder, K., Sachs, R.** Gas flow research at a plane screw type machine model – Part 2. In: Schraubenmaschinen, Forschungsberichte des Fachgebietes Fluidenergiemaschinen Nr. 6, ISSN 0945-1870,pp 20-36, University of Dortmund, 1998
- /7/ **Kauder, K., Sachs, R.** Gas flow research at a plane screw type machine model – Part 3. In: Schraubenmaschinen, Forschungsberichte des Fachgebietes Fluidenergiemaschinen Nr. 7, ISSN 0945-1870, pp 69-80, University of Dortmund, 1999
- /8/ **Sachs, R.** Experimental investigation in clearance flow. dissertation, University of Dortmund, 2002